

Spinning Gluon and Long Range Correlations at RHIC, LHC and EIC

Feng Yuan

Lawrence Berkeley National Laboratory

Guo, Liu, Yuan, Zhu, arXiv: 2406.05880

2/10/25 Guo, Liu, Yuan, arXiv: 2408.14693



EIC Science: from quark/gluon to cosmo

- How do the nucleonic properties such as mass and spin emerge from partons and their underlying interactions?
- How are partons inside the nucleon distributed in both momentum and position space?
- What happens to the gluon density in nucleons and nuclei at small x ? Does it saturate at high energy, giving rise to gluonic matter with universal properties in all nuclei (and perhaps even in nucleons)?
- How do color-charged quarks and gluons, and jets, interact with a nuclear medium? How do confined hadronic states emerge from these quarks and gluons? How do the quark-gluon interactions generate nuclear binding?
- Do signals from beyond-the-standard-model physics manifest in electron-proton/ion collisions? If so, what can we learn about the nature of these new particles and forces?

[EIC Whitepaper for LRP](#)

[QCD Whitepaper, 2303.02579, NPA 2024](#)

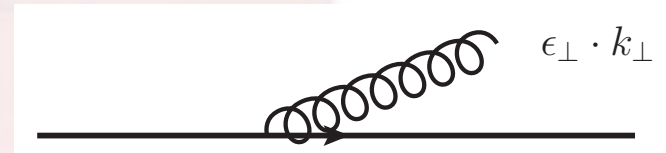


2/10/25

2

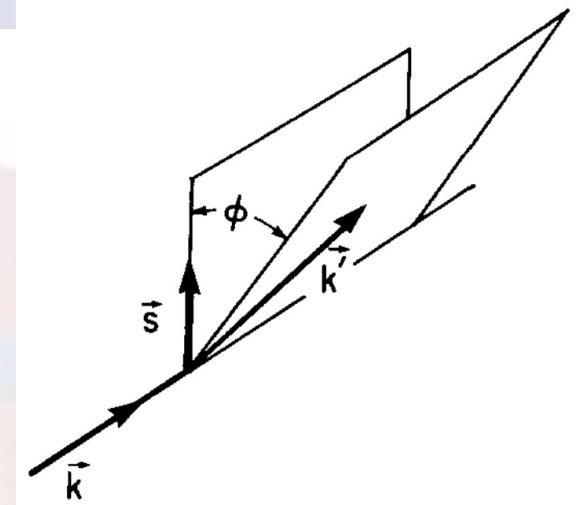
Spinning gluon: nontrivial part of nucleon tomography

- Gluon is always spinning in high energy/small-x
 - Spinning gluon in inclusive DIS
 - Spinning gluon (helicity-flip) in GPD
 - Spinning gluon (linearly polarized) in TMD
- Spinning gluon in Nucleon EEC
 - Two particle correlations in DIS
 - Long range correlation in pp collisions at RHIC and LHC



In the context of inclusive DIS: nuclear gluonometry for $J > 1$

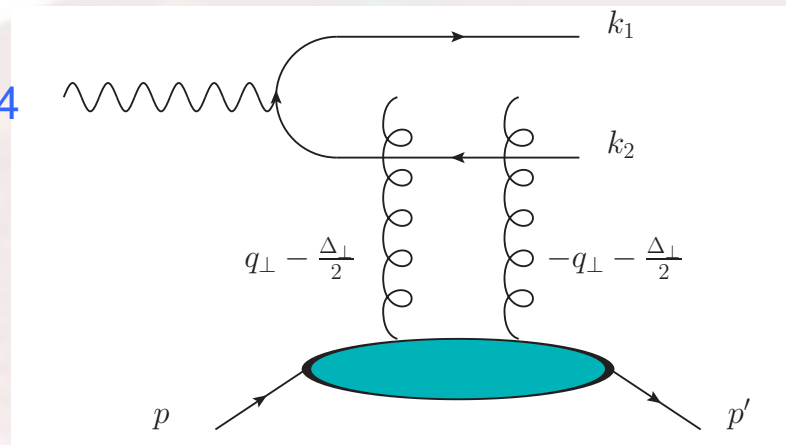
Jaffe, Manohar, 1989



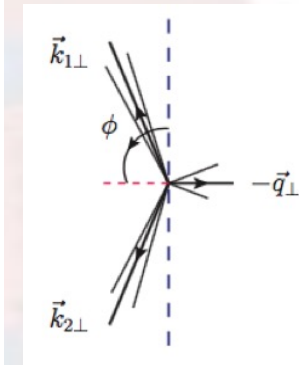
- Structure function difference between polarization along x and y directions, i.e., $\cos(2\phi_S)$ asymmetry
- For nucleons, the asymmetry vanishes in QCD
- Nontrivial asymmetry for nucleus with $J > 1$, e.g., deuteron, only receives contributions from the spinning gluons

Semi-exclusive process: Diffractive Dijet to Probe the Gluon Tomography

Earlier studies:
 Nikolaev, Zakharov 1994
 Bartles, Ewerz, Lotter,
 Wusthoff 1996
 Diehl 1996
 Braun, Ivanov 2005
 ...



Hatta-Xiao-Yuan, 1601.01585



$\cos(2\phi)$
anisotropy

- The diffractive dijet cross section is proportional to the square of the Wigner distribution \rightarrow nucleon/nucleus tomography

$$x\mathcal{W}_g^T(x, |\vec{q}_\perp|, |\vec{b}_\perp|) + 2 \cos(2\phi)x\mathcal{W}_g^\epsilon(x, |\vec{q}_\perp|, |\vec{b}_\perp|)$$

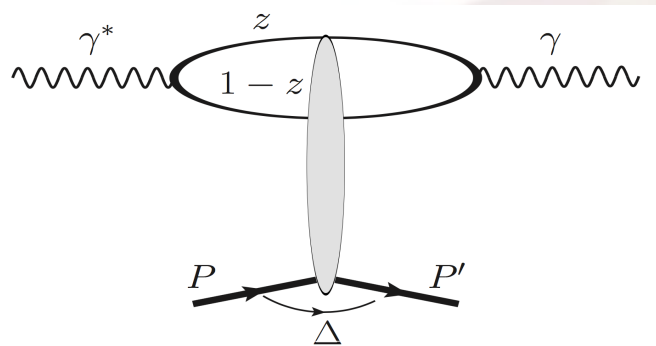
More correlations to study OAM, Spin-Orbital Correlations, ...

Boussarie-Hatta-Bhattacharya, 2022,2024



Spinning gluon in exclusive processes: GPD framework

Hatta-Xiao-Yuan, 1703.02085



Gluon Tomography and Wigner distribution:

$$x\mathcal{W}_g^T(x, |\vec{q}_\perp|, |\vec{b}_\perp|) + 2 \cos(2\phi)x\mathcal{W}_g^\epsilon(x, |\vec{q}_\perp|, |\vec{b}_\perp|)$$

$$\frac{1}{P^+} \int \frac{d\zeta^-}{2\pi} e^{ixP^+\zeta^-} \langle p' | F^{+i}(-\zeta/2) F^{+j}(\zeta/2) | p \rangle$$

$$= \frac{\delta^{ij}}{2} xH_g(x, \Delta_\perp) + \frac{x E_{Tg}(x, \Delta_\perp)}{2M^2} \left(\Delta_\perp^i \Delta_\perp^j - \frac{\delta^{ij} \Delta_\perp^2}{2} \right) +$$

Hoodbhoy-Ji 98
Diehl 01

- A nontrivial tomography distribution of gluon inside the nucleon
- It contributes to a $\cos(2\phi)$ in photon production (DVCS)



Spinning gluon in semi-inclusive process: TMD framework

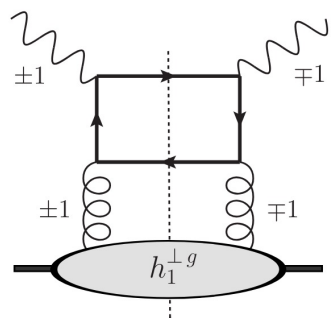
- Linearly polarized gluon distribution

Mulders, Rodrigues, 20021

$$\int \frac{d\xi^- d^2\xi_T}{(2\pi)^3} e^{ik \cdot \xi} \langle P, S | F^{+i}(0) F^{+j}(\xi) | P, S \rangle \left[-g_T^{ij} G(x, \mathbf{k}_T^2) + \left(\frac{k_T^i k_T^j}{M^2} + g_T^{ij} \frac{\mathbf{k}_T^2}{2M^2} \right) H^\perp(x, \mathbf{k}_T^2) \right]$$

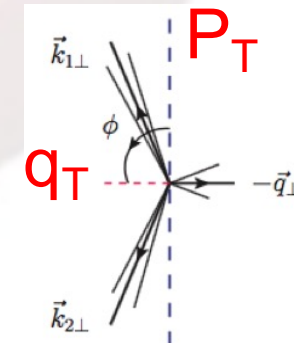
- Can be measured through TMD processes, such as heavy quark pair production in DIS

Boer, Brodsky, Mulders, Pisano, 2011



$$\left[A + \frac{q_T^2}{M^2} B \cos 2(\phi_T - \phi_\perp) \right]$$

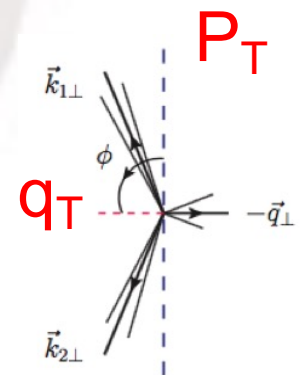
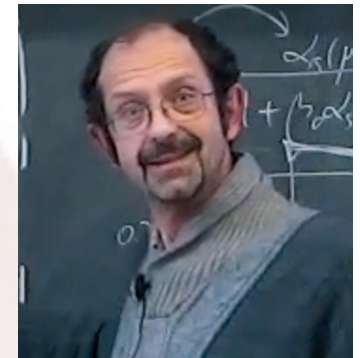
Cos(2φ) between the total and difference of the two leading transverse momenta



2/10/25

Soft gluon radiations can generate and mixes the azimuthal asymmetry

- Azimuthal angular asymmetries arise from soft gluon radiations
 - ϕ is defined as angle between total and different transverse momenta of the two final state particles
- Infrared safe but divergent
 - $\langle \cos(\phi) \rangle$, $\langle \cos(2\phi) \rangle$, ... divergent, $\sim 1/q_T^2$
 - Examples discussed include Vj , top quark pair production



Catani-Grazzini-Sargsyan 2017

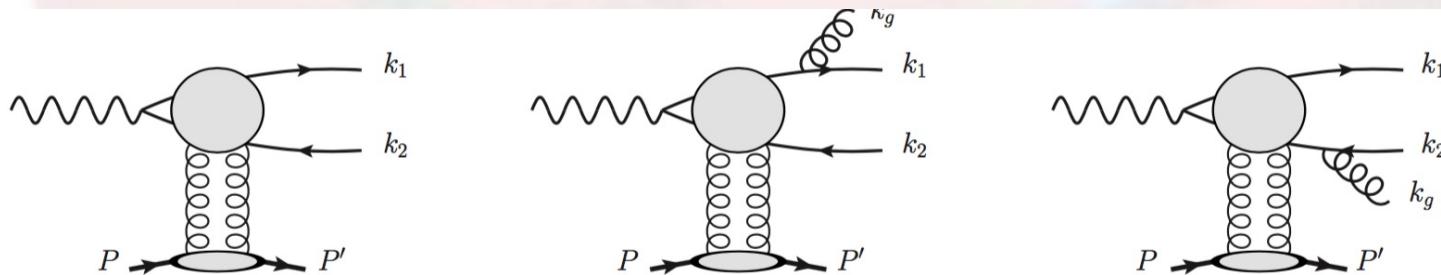
2/10/25

Diffractive dijet production

- Gluon radiation tends to be aligned with the jet direction

$$S_J(q_\perp) = \delta(q_\perp) + \frac{\alpha_s}{2\pi^2} \int dy_g \left(\frac{k_1 \cdot k_2}{k_1 \cdot k_g k_2 \cdot k_g} \right)_{\vec{q}_\perp = -\vec{k}_{g\perp}}$$

$$S_{J0}(|q_\perp|) + 2 \cos(2\phi) S_{J2}(|q_\perp|) + \dots$$



Hatta-Xiao-Yuan-Zhou, 2010.10774, 2106.05307

Leading power contributions, explicit result at α_s

$$S_J(q_\perp) = S_{J0}(|q_\perp|) + 2 \cos(2\phi) S_{J2}(|q_\perp|)$$

$$S_{J0}(q_\perp) = \delta(q_\perp) + \frac{\alpha_0}{\pi} \frac{1}{q_\perp^2}, \quad S_{J2}(q_\perp) = \frac{\alpha_2}{\pi} \frac{1}{q_\perp^2},$$

where

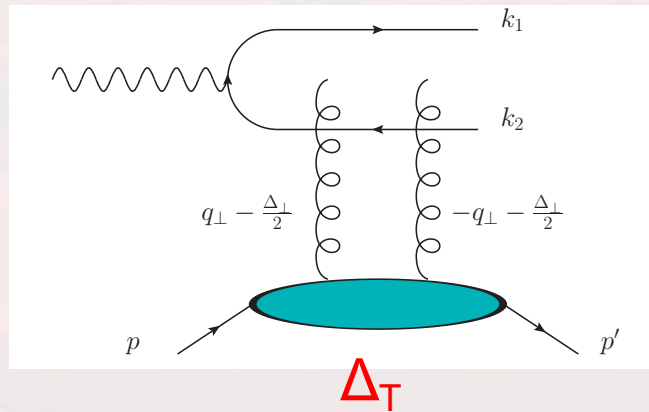
$$\alpha_0 = \frac{\alpha_s C_F}{2\pi} 2 \ln \frac{a_0}{R^2}, \quad \alpha_2 = \frac{\alpha_s C_F}{2\pi} 2 \ln \frac{a_2}{R^2}.$$

a_0, a_2 are order 1 constants, so,

in the small-R limit, $\langle \cos(2\phi) \rangle$ goes to 1

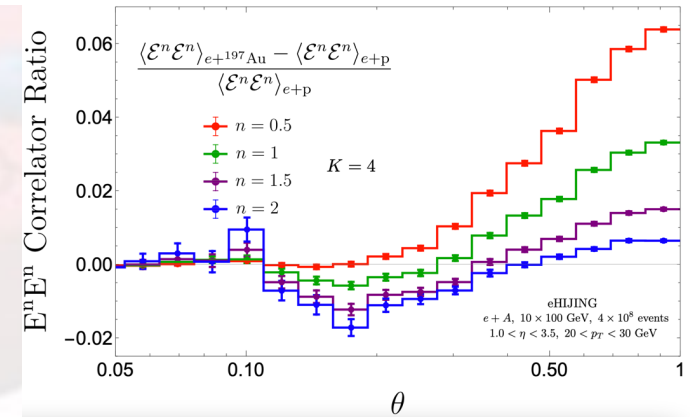
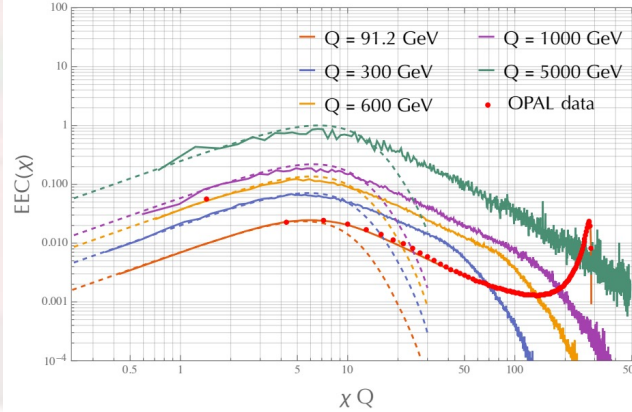
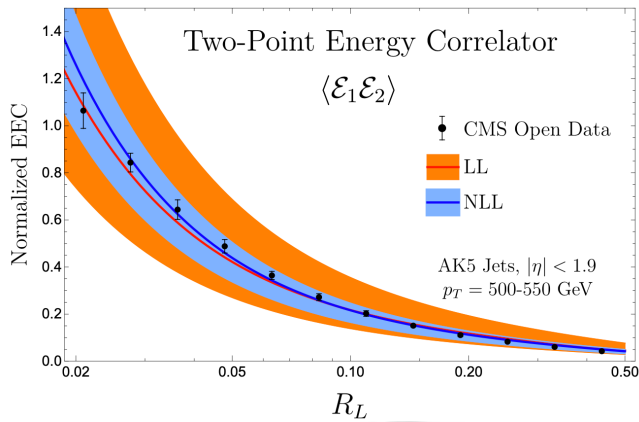
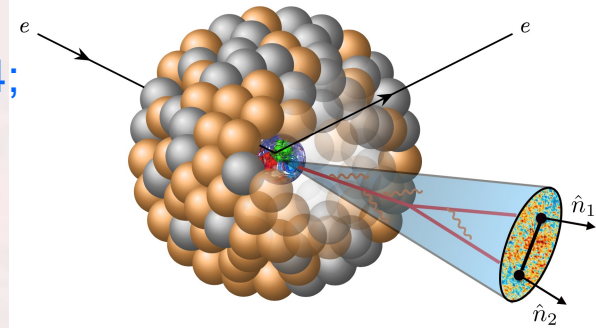
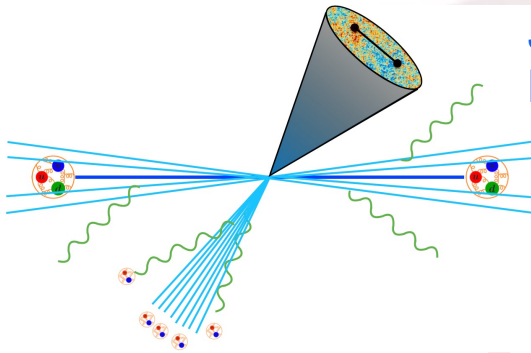
Comments

- To avoid the soft gluon radiation contribution, we need to reconstruct nucleon/nucleus recoil momentum to study the tomography



Energy-Energy Correlators at Colliders

Major focus of recent studies:
 Jet substructure
 Moul, Zhu, Lee, et al, 20-24;



Lee, Mecaj, Moul
 2205.03414

Liu, Vogelsang, Yuan, Zhu
 2/10/25 2410.16371

Devereaux, et al., 2303.08143
 Fu et al., 2411.0486612

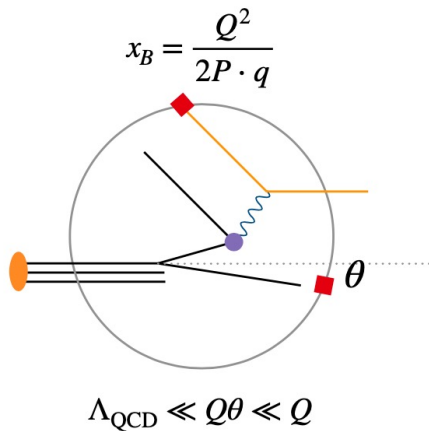


Parton Tomography: Nucleon EEC and DIS

$$f_{q,EEC}(x, \theta) = \int_{-\infty}^{\infty} \frac{dy^-}{2\pi E_P} e^{ixp^+ y^-} \frac{\gamma^+}{2} \langle p | \bar{\psi}(0) \mathcal{E}(\theta) \mathcal{L}\psi(y^-) | p \rangle$$

$$= \sum_X \sum_{i \in X} \frac{E_i}{E_P} \delta(\theta_i^2 - \theta^2) \delta((1-x)p^+ - p_X^+) \frac{\gamma^+}{2} \langle p | \bar{\psi}(0) | X \rangle \langle X | \mathcal{L}\psi(0) | p \rangle$$

Liu, Zhu, 2209.02080
Cao, Liu, Zhu, 2303.01530



$$\Sigma(x_B, Q^2, \theta) = \int \frac{dz}{z} \hat{\sigma}\left(\frac{x_B}{z}, Q^2, \mu\right) f_{\text{EEC}}(z, \theta, \mu)$$

$$\propto \int \frac{dz}{z} \hat{\sigma}\left(\frac{x_B}{z}\right) \frac{1}{\theta^2} \int \frac{d\xi}{\xi} \left(1 - \frac{z}{\xi}\right) P\left(\frac{z}{\xi}\right) [\xi f(\xi)]$$

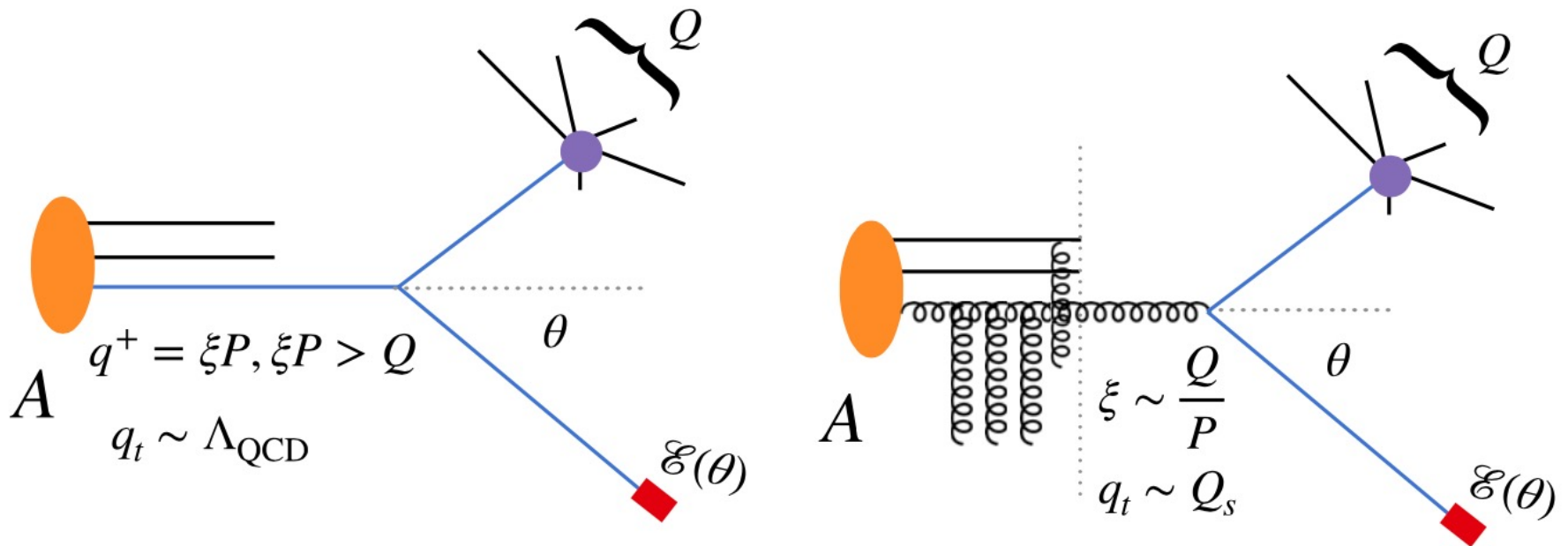
→ Perturbative scaling

- θ -distribution solely determined by f_{EEC}
- In the collinear factorization:
 - $d\Sigma/d \ln \mu = P \otimes \Sigma$, solely determined by the vacuum splitting function
 - $\Sigma \sim \theta^{-2}$ at LO, $\Sigma \sim \theta^{-2+\gamma[\alpha_s]}$ to all orders

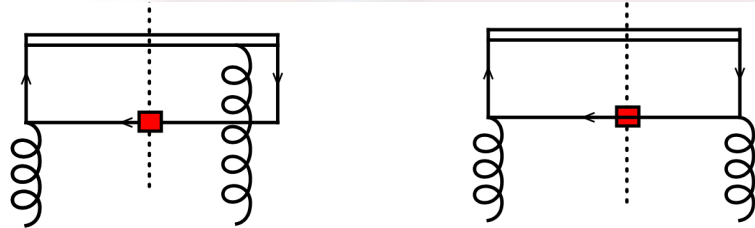
→ All order resummation

LIU/ZH

What happens at small-x



Collinear vs CGC



Collinear:
$$f_{q,\text{EEC}}(x, \theta) = \frac{\alpha_s T_R}{2\pi\theta^2} \int_x^1 \frac{d\xi}{\xi} (1-\xi)(\xi^2 + (1-\xi)^2) \left[\frac{x}{\xi} f_g \left(\frac{x}{\xi} \right) \right]$$

CGC:
$$f_{q,\text{EEC}}(x_B, \theta) = \frac{N_C S_\perp}{8\pi^4} \int d^2 \vec{g}_t \int_{\xi_{\text{cut}}}^1 \frac{d\xi}{\xi} \mathcal{A}_{qg}(\xi, \theta, \vec{g}_t) F_{g,x_B}(\vec{g}_t)$$

$$\mathcal{A}_{qg}(\xi, \theta, \vec{g}_t) = \frac{1}{\theta^2} (1-\xi) \vec{k}_t^2 (\vec{k}_t - \vec{g}_t)^2 \left| \frac{\vec{k}_t}{\xi \vec{k}_t^2 + (1-\xi)(\vec{k}_t - \vec{g}_t)^2} - \frac{\vec{k}_t - \vec{g}_t}{(\vec{k}_t - \vec{g}_t)^2} \right|^2$$

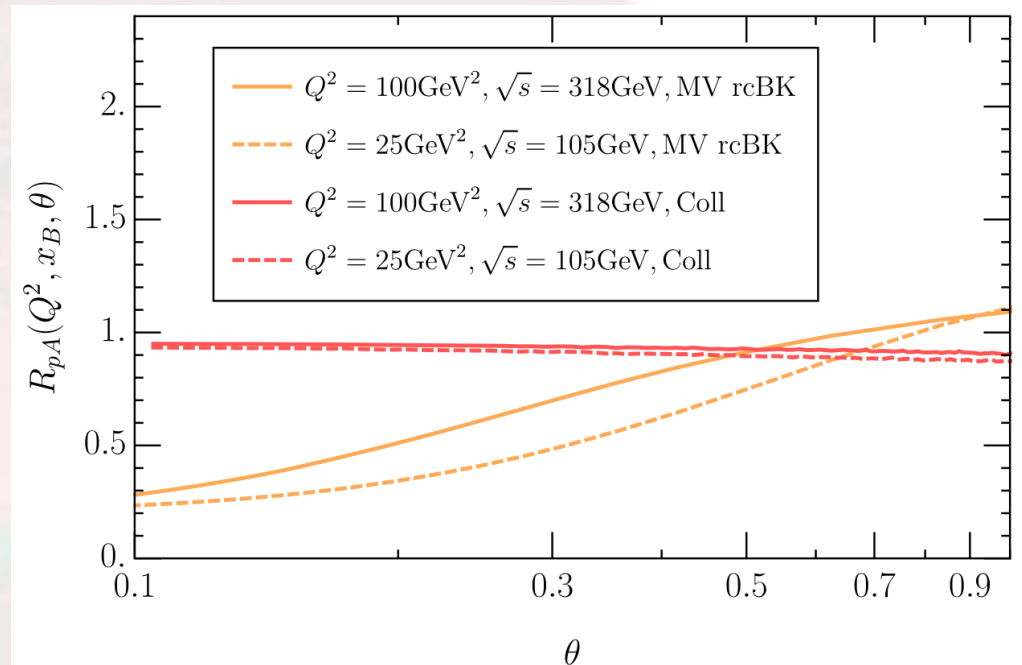
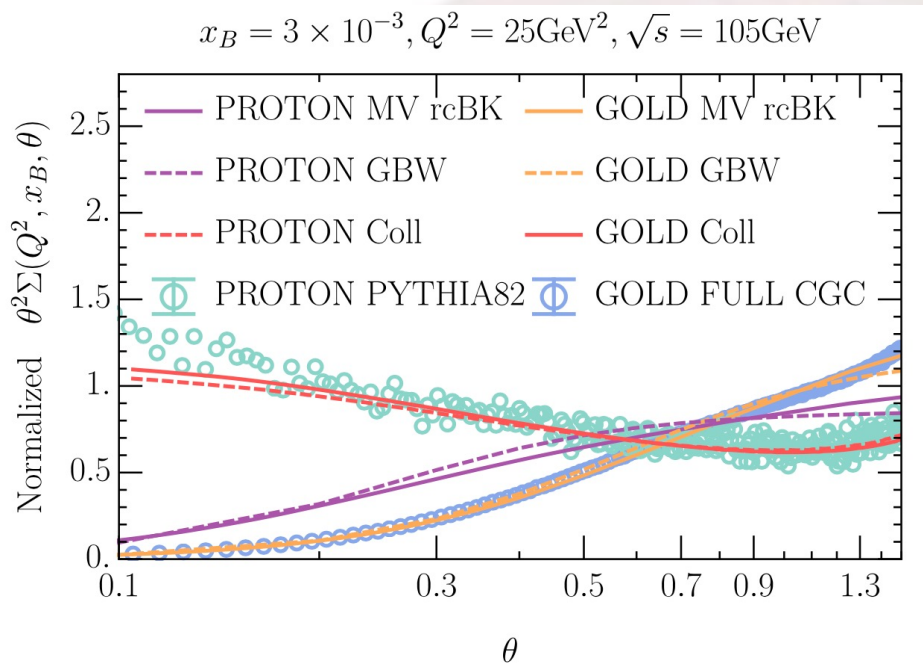
$$k_t = [(1-\xi)/2](Q/2)\theta.$$

2/10/25

See also, NLO: Caucal-Salazar, 2502.02634

15

Gluon saturation modify small- θ behavior



Liu, Liu, Pan, Yuan, Zhu, 2301.01788

2/10/25

16



Spinning gluon in NEEC and two particle $\cos(2\phi)$ correlation in DIS

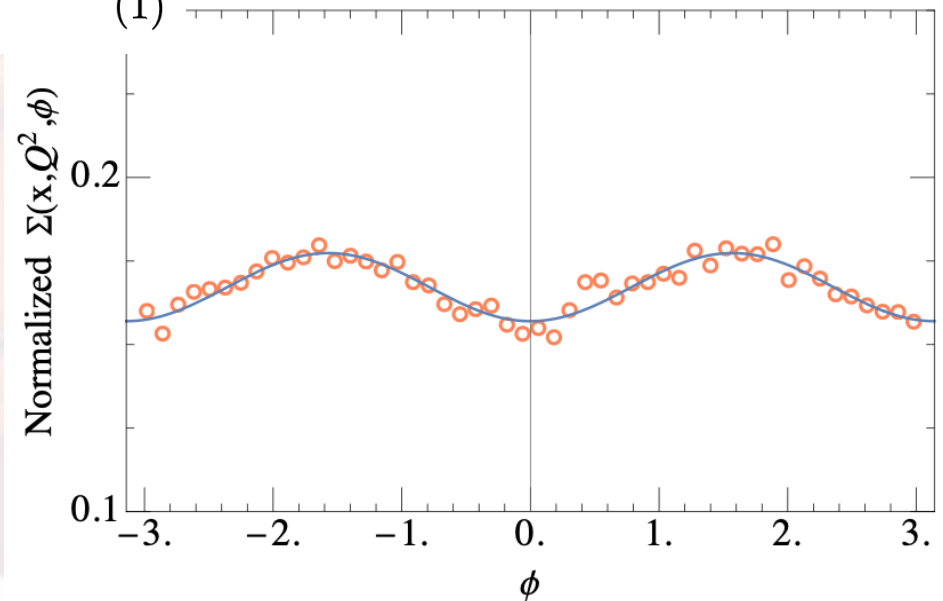
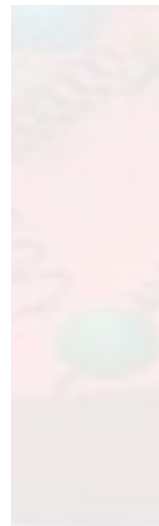
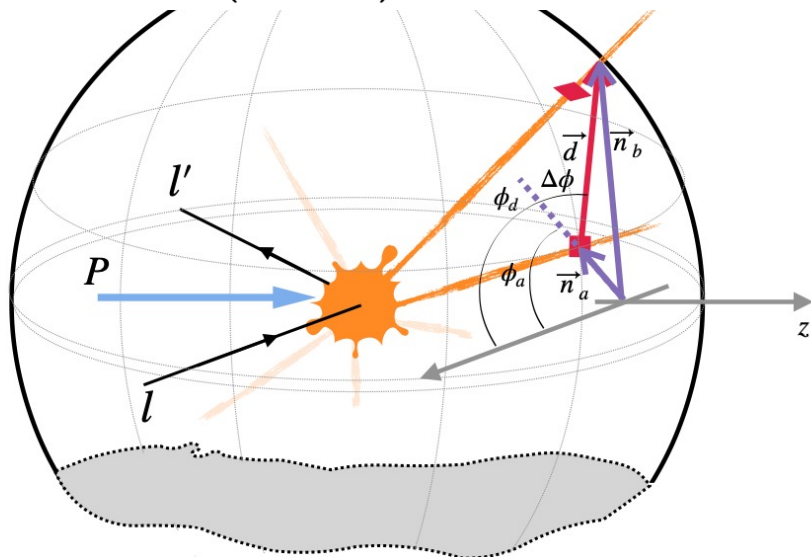
$$f_{g,\text{EEC}}^{\alpha\beta}(x, \vec{n}_a) = \int \frac{dy^-}{2\pi x P^+} e^{-ixP^+ \frac{y^-}{2}}$$

$$\times \langle P | \mathcal{F}^{+\alpha}(y^-) \mathcal{L}^\dagger[\infty, y^-] \hat{\mathcal{E}}(\vec{n}_a) \mathcal{L}[\infty, 0] \mathcal{F}^{+\beta}(0) | P \rangle$$

$$= \left(-g_T^{\alpha\beta} / 2 \right) f_{g,\text{EEC}} + h_T^{\alpha\beta} d_{g,\text{EEC}},$$

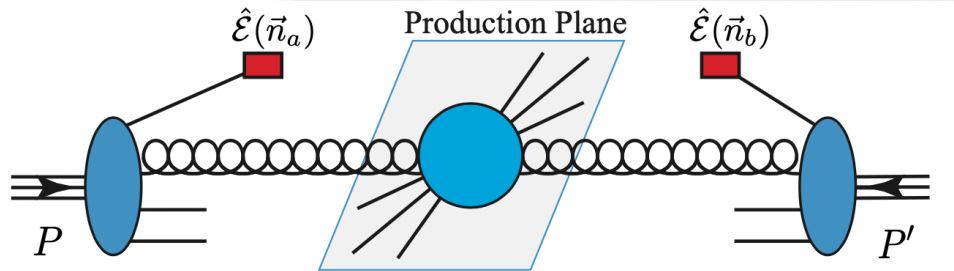
$$h_T^{\alpha\beta} = n_{a,T}^\alpha n_{a,T}^\beta / |n_{a,T}|^2 + \tilde{g}_T^{\alpha\beta} / 2$$

(1)

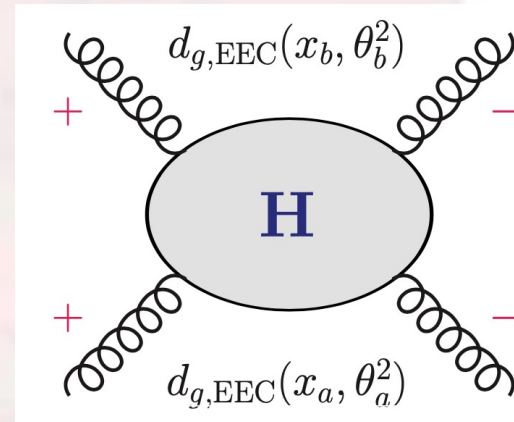


Spinning gluon and long range azimuthal correlation at RHIC and LHC

Guo, Liu, Yuan, Zhu, arXiv: 2406.05880



$$\begin{aligned} & \Sigma(Q^2; \theta_{a,b}, \phi) \\ &= \int d\Omega \left\{ x_a f_{g,\text{EEC}}(x_a, \theta_a^2) x_b f_{g,\text{EEC}}(x_b, \theta_b^2) \hat{\sigma}_0 \right. \\ & \left. + x_a d_{g,\text{EEC}}(x_a, \theta_a^2) x_b d_{g,\text{EEC}}(x_b, \theta_b^2) \hat{\sigma}_2(Q^2) \cos(2\phi) \right\}, \end{aligned} \quad (3)$$



Two examples at the LHC: Higgs, Top quark pair

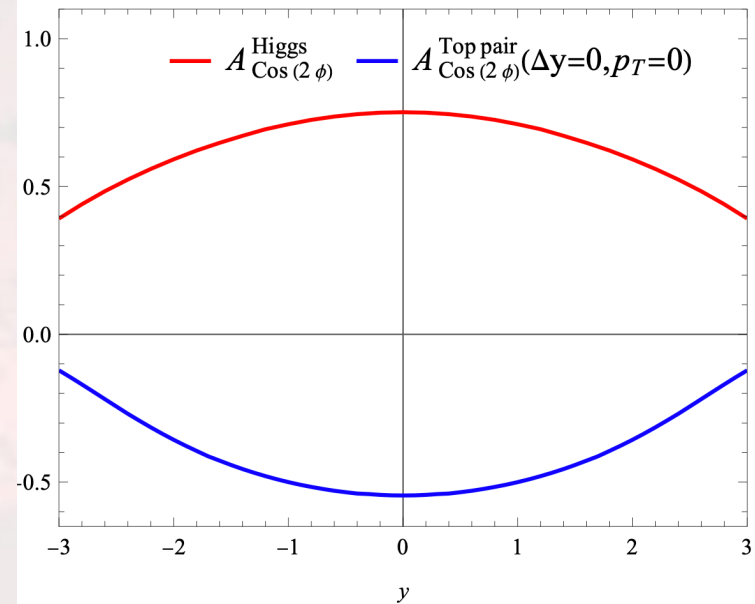
Higgs couples to the spinning gluon directly

$$\hat{\sigma}_2 = \hat{\sigma}_0 = \pi g_\phi^2 / 64$$

Top quark pair is different

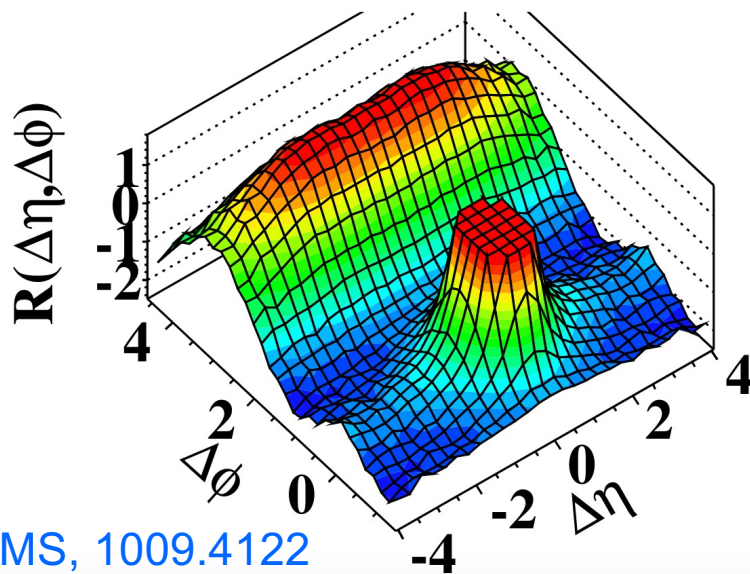
$$\begin{aligned} \hat{\sigma}_0 &= \frac{\alpha_s^2 \pi}{\hat{s}^2} \left[\frac{1}{6} \frac{1}{\hat{t}_1 \hat{u}_1} - \frac{3}{8} \frac{1}{\hat{s}^2} \right] \left[\hat{t}_1^2 + \hat{u}_1^2 + 4m_t^2 \hat{s} - \frac{4m_t^4 \hat{s}^2}{\hat{t}_1 \hat{u}_1} \right] \\ \hat{\sigma}_2 &= \frac{\alpha_s^2 \pi}{\hat{s}^2} \left[\frac{3}{8} \frac{1}{\hat{s}^2} - \frac{1}{6} \frac{1}{\hat{t}_1 \hat{u}_1} \right] \frac{2m_t^4 \hat{s}^2}{\hat{t}_1 \hat{u}_1}, \end{aligned} \quad (7)$$

Cos(2φ) asymmetries for Higgs and top pair at $\sqrt{s}=13$ TeV



Extension to multi-jet production: ridge phenomena in pp collisions

(d) CMS $N \geq 110$, $1.0 \text{ GeV}/c < p_T < 3.0 \text{ GeV}/c$



First step, understand EEC:

$$\begin{aligned} \Sigma^{jet}(Q^2; \theta_{a,b}, \phi) &= \sum_{ij} \int d\sigma^{jet}(Q^2) \frac{E_i}{E_P} \frac{E_j}{E_P} \mathcal{F}(\phi; \vec{n}_{a,b}) \\ &\quad \times \delta(\vec{n}_a - \vec{n}_i) \delta(\vec{n}_b - \vec{n}_j), \quad (1) \\ &= \int d\Omega \{ x_a f_{g,EEC}(x_a, \theta_a^2) x_b f_{g,EEC}(x_b, \theta_b^2) \hat{\sigma}_0 \\ &\quad + x_a d_{g,EEC}(x_a, \theta_a^2) x_b d_{g,EEC}(x_b, \theta_b^2) \hat{\sigma}_2(Q^2) \cos(2\phi) \} \end{aligned}$$

CMS, 1009.4122

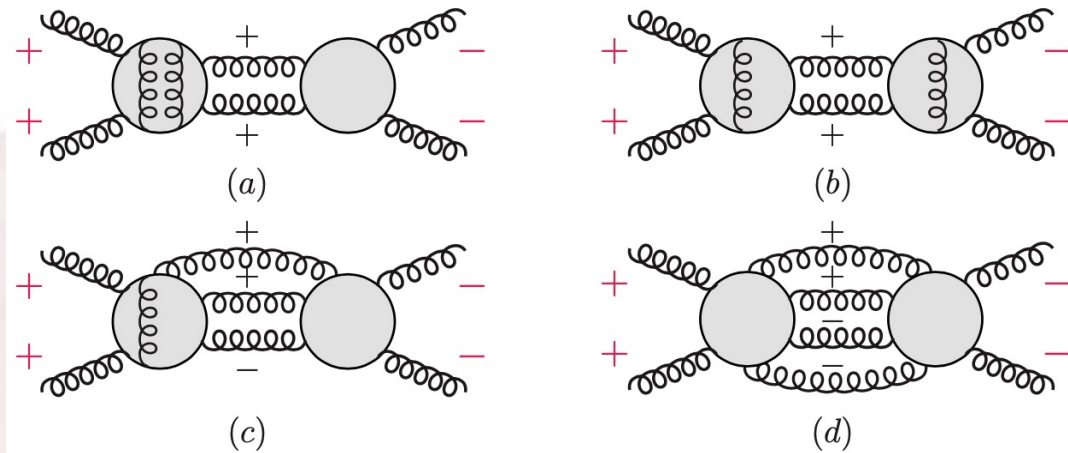


Cos(2φ) and helicity amplitudes in QCD

$$\hat{\sigma}_2 \propto \sum_{\lambda_3 \lambda_4} \mathcal{A}(\pm, \pm, \lambda_3, \lambda_4) \mathcal{A}^*(\mp, \mp, \lambda_3, \lambda_4)$$

- Cos(2φ) comes from interference between double helicity-flip with the same helicity for the incoming gluons
- QCD amplitude vanishes for same helicity for all external partons or only one has different helicity Parke, Taylor, 1986
Berends, Giele, 1988
- Any combinations of λ_3 and λ_4 the above vanishes, and one-loop amplitude contribution also vanishes Bern, Kosower, 1992;
- **Nonvanishing contribution only comes from two-loop amplitudes** ...

A power counting rule



- Similar conclusion holds for three jet final state, vanishing at the leading order, but survives at NLO
- Four jet final state, $\cos(2\phi)$ is leading order

Number of Jets	2	3	≥ 4
$\langle \cos(2\phi) \rangle$ asymmetry	$\mathcal{O}(\alpha_s^2)$	$\mathcal{O}(\alpha_s)$	$\mathcal{O}(1)$

Dijet $\cos(2\phi)$ at NNLO

- Applying the two-loop amplitudes [Ahmed, Henn, Mistlberger, 1910.06684;](#)

[Caola, Chakraborty, Gambuti, von Manteuffel, Tancredi, 2112.11097](#)

$$\begin{aligned}\hat{\sigma}_2^{(2)} &= A^{(1)}(+++-)A^{(1)*}(- - + -) \\ &+ A^{(1)}(++++)A^{(1)*}(- - ++) \\ &+ A^{(2)}(++++)A^{(0)*}(- - ++) + h.c.\end{aligned}$$

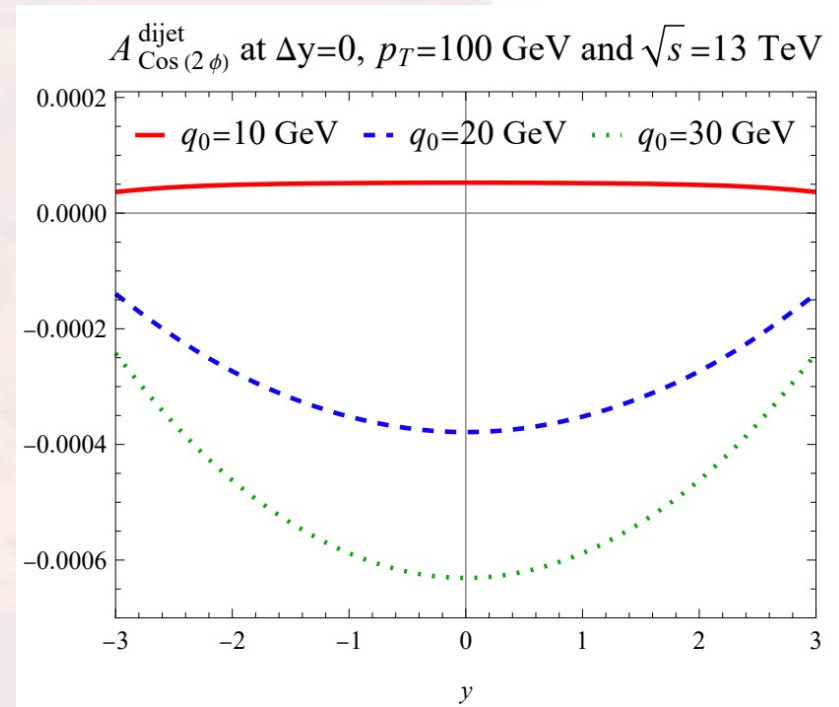
- There are IR divergences, which will be cancelled by soft real gluon radiation (with a jet veto q_0)

$$\begin{aligned}\hat{\sigma}_2^{(2)} &= \hat{\sigma}_{2,0}^{(2)}(x) \ln \left(\frac{\hat{s}}{q_0^2} \right) + \hat{\sigma}_{2,2}^{(2)}(x) \\ &- \hat{\sigma}_{2,1}^{(2)}(x) \left[\mathcal{P}_{gg}^d \otimes d_g(x_a) + \mathcal{P}_{gg}^d \otimes d_g(x_b) \right]\end{aligned}$$

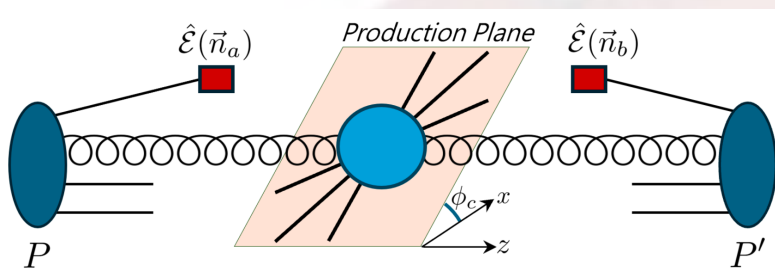
21/10/23

Phenomenological results

- Suppressed by $(\alpha_s/4\pi)^2$, order 10^{-4} - 10^{-3}
 - Roughly same order as that found in the long range ridge for lower end of multiplicity events
- Strongly depends on the jet veto q_0



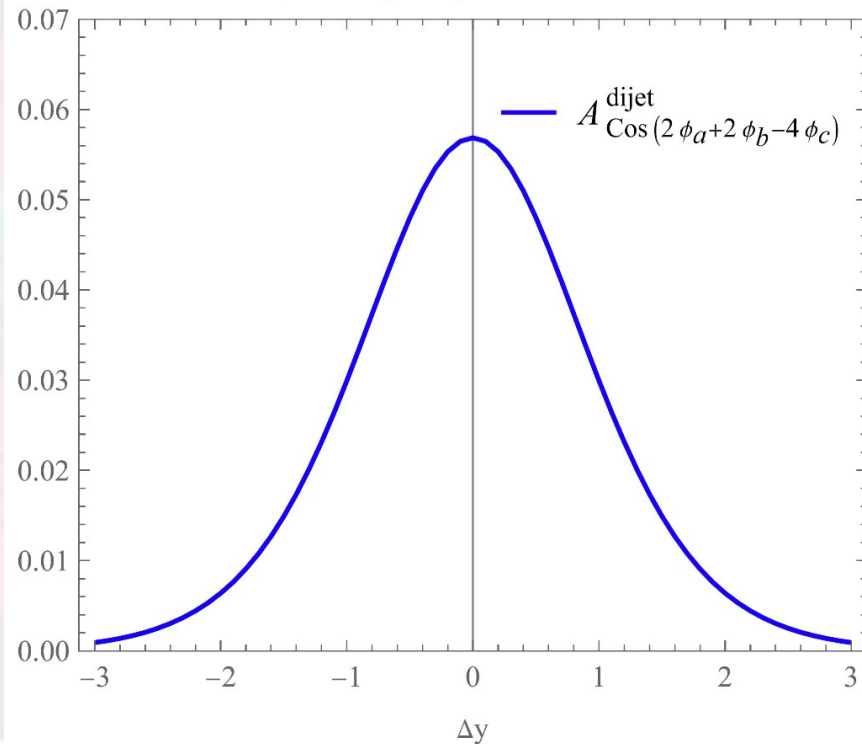
Cross check with semi-long range correlation



$$\langle \cos(2\phi_a + 2\phi_b - 4\phi_c) \rangle_{\text{dijet}}$$

$$= \frac{\int d\Omega d_{g,\text{EEC}}(x_a) d_{g,\text{EEC}}(x_b) \frac{9}{2} \frac{\hat{s}^2 + \hat{t}^2 + \hat{u}^2}{2\hat{s}^2}}{\int d\Omega f_{g,\text{EEC}}(x_a) f_{g,\text{EEC}}(x_b) \frac{9}{2} \frac{(\hat{s}^2 + \hat{t}^2 + \hat{u}^2)^3}{8\hat{s}^2 \hat{t}^2 \hat{u}^2}}$$

y-integrated $A_{\text{Cos}(2\phi_a+2\phi_b-4\phi_c)}^{\text{dijet}}$ at $\sqrt{s}=13$ TeV and $P_T=100$ GeV





Next step

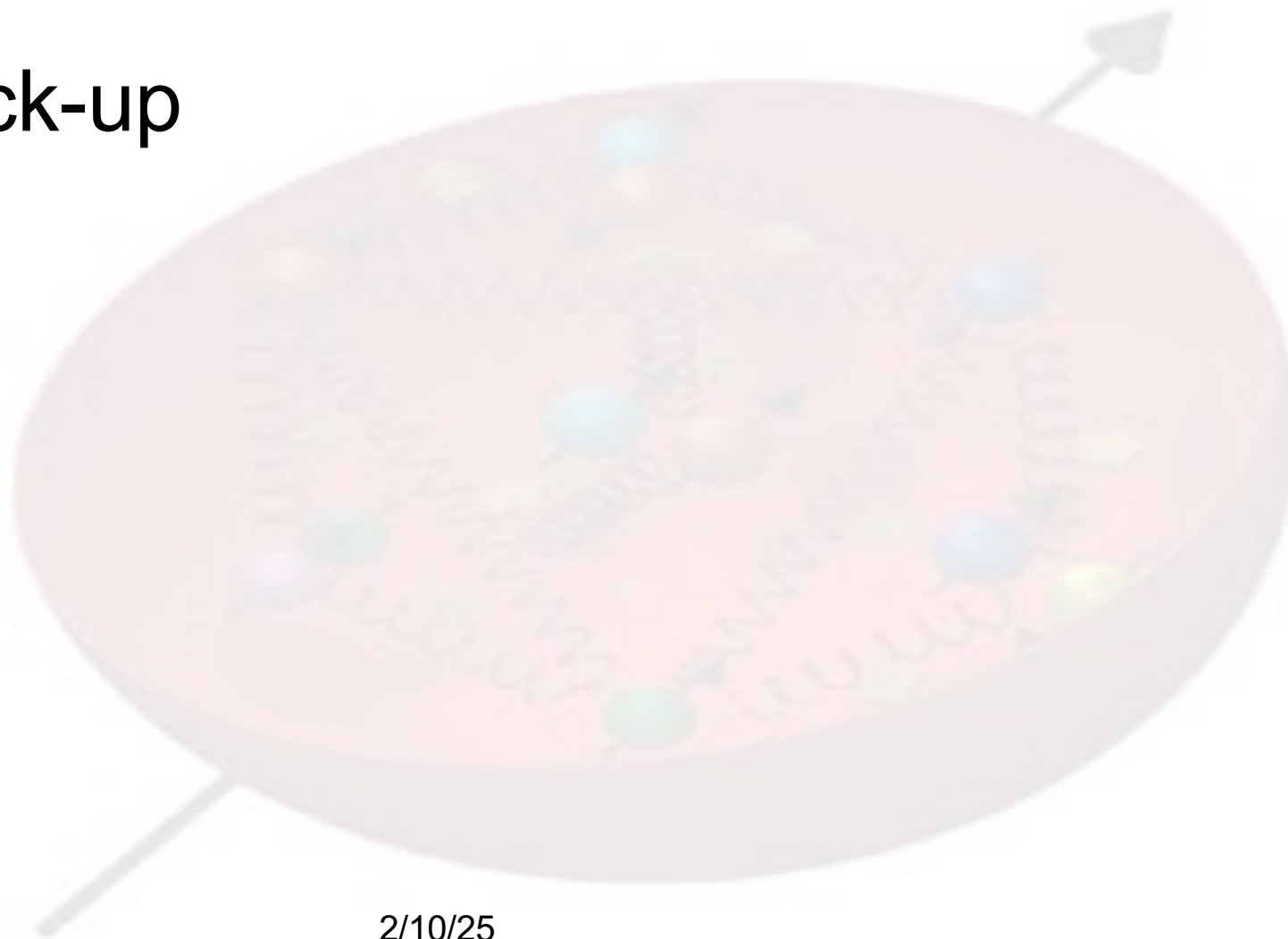
- Compute three-jet, four-jet asymmetry
 - one-loop amplitudes for three-jet final state
 - tree amplitudes for four-jet final state
- Build simulation for the ridge measurements
 - Keep interference and spin information in the parton shower simulations
 - And/or include high number of jets in the final states



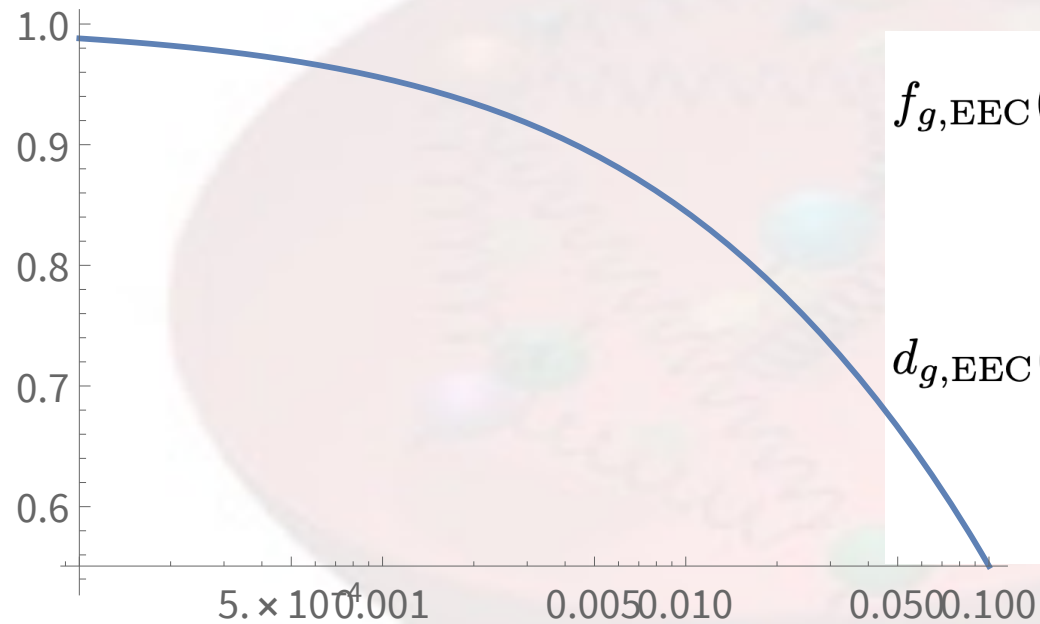
Conclusion

- Spinning gluon is an important aspect of nucleon tomography, in particular, at small- x
- We should be able to observe the long range azimuthal angular correlations due to the spinning gluon effects
- Extension to the spinning quark should be pursued as well

Back-up



Gluon is spinning at small-x



$$f_{g,\text{EEC}}(x, \theta_a^2) = \frac{\alpha_s}{2\pi} \frac{1}{\theta_a^2} \int_x^1 \frac{dz}{z} \frac{x(1-z)}{z} \times \left[\mathcal{P}_{g/q}(z) f_q\left(\frac{x}{z}\right) + \mathcal{P}_{g/g}(z) f_g\left(\frac{x}{z}\right) \right]$$

$$d_{g,\text{EEC}}(x, \theta_a^2) = \frac{\alpha_s}{2\pi} \frac{1}{\theta_a^2} \int_x^1 \frac{dz}{z} \frac{x(1-z)}{z} \times \frac{2(1-z)}{z} \left[C_F f_q\left(\frac{x}{z}\right) + C_A f_g\left(\frac{x}{z}\right) \right]$$

Universal IR Structure in QCD Amplitudes

Catani 1998; Sterman-Tejeda-Yeomans 2003

$$\mathbf{I}^{(1)} \equiv \left[- \sum_i \left(\frac{\gamma_K^{[i](1)}}{2\epsilon^2} + \frac{\mathcal{G}_0^{[i](1)}}{\epsilon} \right) \mathbf{1} + \frac{\mathbf{\Gamma}^{(1)}}{\epsilon} \right] \left(-\frac{\mu^2}{s} \right)^\epsilon \quad \mathbf{\Gamma}^{(1)} = \frac{1}{2} \sum_i \sum_{j \neq i} \mathbf{T}_i \cdot \mathbf{T}_j \ln \left(\frac{-\mu^2}{s_{ij}} \right)$$

■ Applying in our case

$$\hat{\sigma}_2^{(2)v} = \frac{1}{\epsilon} \left(\hat{\sigma}_{2,J}^{(2)v} + \hat{\sigma}_{2,S}^{(2)v} \right) \begin{cases} \hat{\sigma}_{2,S}^{(2)v} = \frac{2}{\mathcal{V}} \langle A^{(1)}(+ + + +) | 2\text{Re} [\mathbf{\Gamma}^{(1)}] | A^{(0)}(- - + +) \rangle \\ \hat{\sigma}_{2,J}^{(2)v} = - \sum_i \gamma_K^{[i](1)} \hat{\sigma}_2^{(1)\epsilon} = -8C_A \hat{\sigma}_2^{(1)\epsilon} \end{cases}$$

Helicity amplitudes can be found in Refs. for two loop results:

Ahmed, Henn, Mistlberger, 1910.06684;

Caola, Chakraborty, Gambuti, von Manteuffel, Tancredi, 2112.11097